Nanoparticle Coatings for Enhanced Capture of Flowing Cells in Microtubes

Woojin Han,[†,⊥] Bryce A. Allio,[†,⊥] David G. Foster,[‡,*] and Michael R. King[§]

[†]Department of Biomedical Engineering, [‡]Department of Chemical Engineering, University of Rochester, Rochester, New York 14627, and [§]Department of Biomedical Engineering, Cornell University, Ithaca, New York 14853. [⊥]These authors contributed equally to this work.

ABSTRACT Recently, a flow-based selectin-dependent method for the capture and enrichment of specific types of cells (CD34+ hematopoetic stem and progenitor cells and human leukemia HL60) from peripheral blood was demonstrated. However, these devices depend on a monolayer of selectin protein, which has been shown to have a maximum binding efficiency as a function of surface area. A novel surface coating of colloidal silica nanoparticles was designed that alters the surface roughness resulting in increased surface area. The nanoparticles were adhered using either an inorganic titanate resinous coating or an organic polymer of poly-L-lysine. Using Alexa Fluor 647 conjugated P-selectin, an increase in protein adsorption of up to 35% when compared to control was observed. During perfusion experiments using P-selectin-coated microtubes, we observed increased cell capture and greatly decreased rolling velocity at equivalent protein concentration compared to nonparticle control. Atomic force microscopy showed increased surface roughness consistent with the nanoparticle mean diameter, suggesting a monolayer of particles. These results support the coating's potential to improve existing cell capture implantable devices for a variety of therapeutic and scientific uses.

KEYWORDS: nanoparticles · poly-L-lysine · P-selectin · KG1a · titanium(IV) butoxide · nanoparticle coating · adhesive

Biomaterial surface topography has been shown to influence leukemic cell behavior as well as protein adsorption to material surfaces.[1−12] The rapid and inexpensive production of nanotopography on surfaces intended for biological interfaces has received much attention in applications such as nanoprinting, fibroblast, and tumor cell adhesion.[7−12,16−18] Colloidal silica coupled with the use of commercial or biological adhesives is an attractive prospect for achieving highly structured silica nanotopography.

A wide range of biological uses requires an equally large range of environmental conditions motivating the investigation of a variety of adhesives. In particular, organic titanate has long been used as an industrial adhesive; considering that titanium oxide surfaces have been found to be nonimmunogenic, these adhesives are attractive as colloidal silica immobilizers for biological applications.[16−19] In addition, previous studies have demonstrated the influence of poly-L-lysine (PLL) on colloidal silica assembly and condensation, via electrostatic interactions of negatively charged silica particles and ammonium groups of PLL.[20]

Recently, a flow-based selectin-dependent method for the capture and enrichment of specific types of cells from peripheral blood was demonstrated.[1,2,21] These devices use selectin proteins that are essential for leukocyte rolling in the inflammation cascade. Products of inflammation trigger the presentation of P-selectin on the lumen of blood vessels. P-selectin (sP) in concert with margination caused by blood flow produces an environment where leukocytes are recruited to roll along the vessel wall. In experimental devices, cells interact with commercially available recombinant chimeric sP conjugated with the Fc region and slowly roll in the direction of an applied shear stress or become completely immobilized. These devices depend on a monolayer of selectin protein, which has been shown to have a maximum binding efficiency as a function of surface area, and are good candidates for manipulation of surface nanotopography.

Several methods are currently used for the detection and isolation of circulating tumor cells (CTC) from blood.[22,23] Most methods start with a Ficoll density gradient centrifugation to separate the nucleated cells (including leukocytes and CTC) from the majority of red blood cells, platelets, and serum. One approach to isolate epithelial-type CTC from Ficoll-extracted cells is to perform immunoprecipitation (e.g., via magnetic beads) with antibodies against the EpCAM surface marker.[24] Another approach is to take the nucleated cells and flow these through a filter with pore size ≥8 μm, which can be useful for isolating CTC that are larger than leukocytes (e.g., iso-
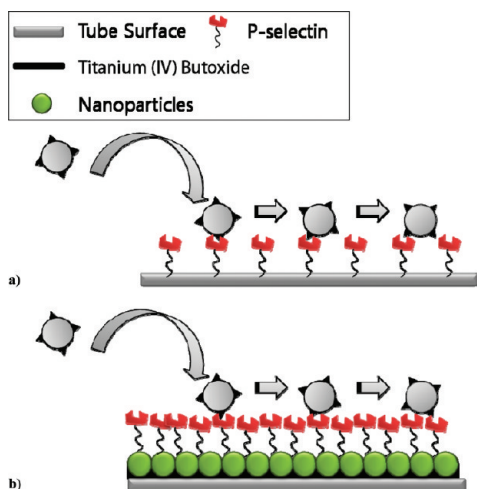
Figure 1. (a) Representation of control tube containing only P-selectin and rolling cells. (b) Representation of NP tube creating increased binding surface for P-selectin.

lation by size of epithelial tumor cells, or ISET, Metagenex, Paris, France). Examination of the resulting filtrate, potentially after immunofluorescent labeling, can be useful for visually identifying circulating tumor microemboli (CTM) on the filter surface.[25] The most commonly used method for detection of CTC in blood is to take the cells extracted from Ficoll separation, lyse the cells, and isolate mRNA, and then perform reverse transcriptase polymerase chain reaction (RT-PCR) to amplify mRNA for epithelial markers such as cytokeratin 19/20 (CK19, CK20), carcinoembryonic antigen (CEA), and prostate-specific antigen (PSA). This is a remarkably sensitive assay and can routinely achieve detection sensitivities down to 1 cell per blood sample of whole blood. The drawbacks of RT-PCR detection of CTC are that (1) the CTC are destroyed prior to RNA extraction so CTM cannot be identified and cells cannot be expanded in culture, (2) the potential exists for both false negative and false positive detection due to the lack of epithelial markers on 30% of CTC[26] and positive labeling for epithelial markers on blood cells in $5-15\%$ of normal patients.[22] A recent study using microfluidic posts to isolate CTC from blood alleviates some of these limitations by acquiring intact, viable cells[27] but is also based on antibodies against the EpCAM epithelial surface marker so is also limited to the ~70% of the CTC types which have not lost their epithelial markers prior to intravasation. As we have recently reported, cancer cell adhesion *via* selectin-coated surfaces represents a promising alternative,[28] capable of isolating viable, intact tumor cells from patient blood samples.

In this study, both organic and inorganic adhesive layers were used to form a colloidal silica nanoparticle (NP) interface layer as a means to improve cell capture (Figure 1). Silica NP presence on modified surfaces was evaluated by atomic force microscopy (AFM). Immunofluorescence microscopy of P-selectin was used to assess the surface quantity of P-selectin. An acute mye-

loid leukemia cell line (KG1a) was used for cell adhesion assays due to their high expression of P-selectin glycoprotein ligand-1 (PSGL-1), which mediates cell rolling on P-selectin both *in vitro* and *in vivo*.[22−25]

RESULTS AND DISCUSSION

AFM Analysis. The AFM image of NP-treated surfaces confirmed the presence of NPs even after thorough washing (Figure 2). In addition, the AFM images show topography of increased surface roughness as well as surface area. The control (adhesive only: PLL layer only, titanium(IV) butoxide layer only) surfaces show minimal roughness compared to the NP-treated surfaces.

Immunofluorescence Quantification of P-Selectin. Immunofluorescence of labeled P-selectin was used to compare surfaces and examine the NP layer's ability to increase the surface area or quantity of adsorbed selectin. The average fluorescence intensity of CD62P-Alexa Fluor 647 conjugated anti-P-selectin on NP surfaces indicated significantly higher intensity than the control surface (Figure 3). On average, P-selectin adsorption to NP surfaces was increased up to 35% compared to control. No significant difference was observed between the two NP surfaces prepared with PLL and titanium(IV) butoxide as adhesives ($P > 0.05$). The enhanced P-selectin adsorption from increased surface roughness results in more PSGL-1 ligands binding CD34+ cell surface receptors of a given amount of cells introduced to the system. Potentially, titration of P-selectin NPs with neutral NPs would support flexibility of the nanoparticle system for controlling surface ligand density.

Nanoparticle Coatings Using Poly-L-lysine as an Adhesive. Once PLL is absorbed and coated onto the tube surface, the number of positively charged ammonium groups present on PLL increases, which then attract negatively charged colloidal silica *via* electrostatic interactions (Figure 4).[17] Furthermore, it is important to note that confinement can affect the diffusion coefficient of NPs, which may lead to particle aggregation.[26,27] Unwanted confinement that favors particle aggregation can be created as the silicate layer coating becomes thicker. Tubes can become occluded by the buildup of NP aggregation; therefore, it is crucial to avoid introduction of excessive NPs inside the PLL-coated tubes.

To gain a better understanding of the PLL adhesive layer, the coating thickness was determined by measuring the mass differences between completely desiccated 50 cm long coated and uncoated tubes. On the basis of 10 independently conducted trials ($n = 10$), the average mass difference was measured as 0.80 ± 0.03 mg. Using these data and the reported density of PLL, the coating thickness was calculated to be 151 ± 6 nm, which is in remarkable agreement with the reported random coil (at neutral pH) PLL cylinder dimensions of $\sim 5 \times 300$ Å $= 150$ nm after absorption.[28−30] Thus, this
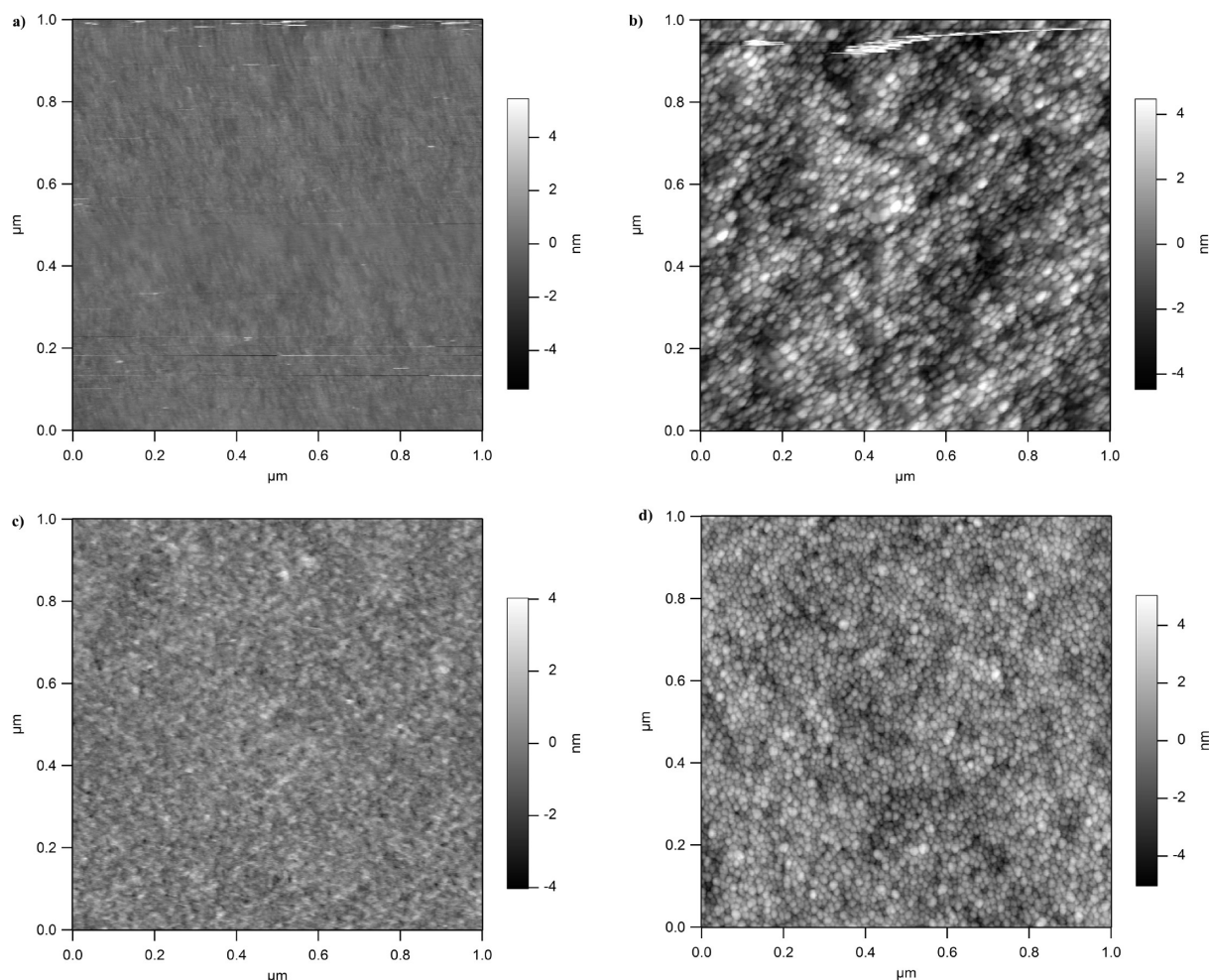
Figure 2. (a) AFM image of control (adhesive only) titanium(IV) butoxide surface. **(b)** AFM image of immobilized NPs on titanium(IV)-butoxide-treated surface. **(c)** AFM image of control (adhesive only) PLL surface. **(d)** AFM image of immobilized NPs on titanium(IV)-butoxide-treated surface.

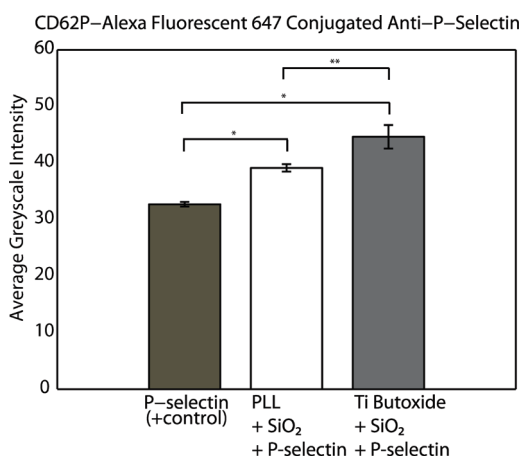indicates that PLL adheres the NPs while maintaining a very thin and reproducible average coating surface.

Figure 3. Average gray scale intensity of Alexa Fluor 647 conjugated anti-P-selectin. The background fluorescence of the tube has been subtracted from each measurement. Both NP-coated surfaces showed significantly higher intensity than the control. No significant difference was observed between the two NP surfaces: $*P < 0.05$; $**P > 0.05$.

Other advantages of PLL as the NP coating adhesive include its biocompatibility and water solubility during processing. PLL is a polypeptide widely used in mammalian cell culture to coat culture surfaces to promote nonspecific cell adhesion and spreading.[14] Thus, PLL is a promising adhesive that can be used when designing an implantable biomedical device in the future.

Characteristics of cell rolling and adhesion have been shown to be effective means of evaluating surface topography on the nanoscale.[4] To study the effects of a NP interface on the capture of flowing cells, rolling experiments comparing NP-coated tubes and control tubes were performed. A significantly slower rolling velocity of KG1a cells on the NP surface produced using PLL and silica NPs compared to KG1a cells on the control surface was observed (Figure 5). Over the entire range of wall shear stresses studied, the mean rolling velocities of cells were significantly slower in the NP-coated tubes ($P < 0.05$). Similarly, the total number of cells captured in a NP-coated tube was significantly greater than with the control device lacking the NP layer (Figure 6). At a wall shear stress of 2 dyn/cm², the
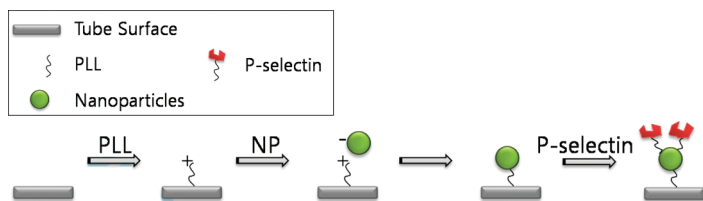
Figure 4. Presence of PLL on the surface allows for the opportunity of electrostatic interactions between the surface and the NPs.

NP-coated device showed up to a 100% increase in the total number of cells captured relative to the non-NP device (Figure 7).

PLL is a biological macromolecule that is used to coat synthetic surfaces to promote nonspecific spreading and adhesion of anchorage-dependent cells.[31−33] To eliminate the possibility of undesired nonspecific cell adhesion to PLL that could influence the cell capture behavior, a similar experiment was conducted with different negative controls (no P-selectin incubation, blocked with 5% BSA), PLL and PLL with NP-coated surfaces. Both negative control tubes showed no nonspecific cell adhesion under a wall shear stress of 2 dyn/cm^2 (Figure 8). This result indicates that PLL is exclusively acting as a NP-immobilizing adhesive and not contributing to the enhancement of cell capture though nonspecific electrostatic interactions. In addition, this supports the conclusion that the NP-coated surface with P-selectin significantly improves the cell capture from its increased surface roughness and area.

The desire to make comparisons with as homogeneous sample as possible was a motivating factor for the use of a cultured cell line instead of primary human blood cells. It was determined in a previous flow cytometry study that this cell line has a narrow distribution of cell diameters (25% total variation) and selectin ligand surface expression (50% total variation). Primary peripheral blood cells collected from human volunteers typically exhibit variability in cell size and receptor expression much greater than this, producing results which are harder to interpret. In addition, this requires the averaging of many donor samples. In the previous work, it has been found that, for heterogeneous cell samples, the focus is shifted simultaneously to a smaller subpopulation, toward the tail of a Gaussian distribution.[34]

Nanoparticle Coatings Using Titanium(IV) Butoxide as an Adhesive. The coating thickness of the titanium(IV) butoxide adhesive layer was determined *via* the same method as described for the PLL coating thickness calculation above. On the basis of 10 independently conducted trials ($n = 10$), the average mass difference equaled 1.75 ± 0.43 mg. From this, the coating thickness was calculated to be 196.2 ± 5.4 nm. The same concentration of titanium(IV) butoxide coating yielded a slightly thicker layer compared to the PLL coating, but still a very thin adhesive layer for successful NP immobilization.

Using KG1a cells, the rates of cell adhesion and rolling were evaluated for cells flowing over NPs immobilized by titanium(IV) butoxide and functionalized with P-selectin. Over the entire range of P-selectin concentration studied, the presence of NPs on the interior lumen of the flow device showed significantly greater cell capture at a wall shear stress of 2 dyn/cm^2 (Figure 9). Specifically, the NP surface showed similar cell capture rates as the control surface at over $1.5\times$ less concentrated P-selectin incubation concentration. Surfaces of adhesive only (BSA blocked), as well as surfaces of adhesive and NPs (BSA blocked), were tested and showed no significant cellular adhesion or rolling. This result further indicates that the NP and titanium(IV) butoxide adhesive layer alone do not
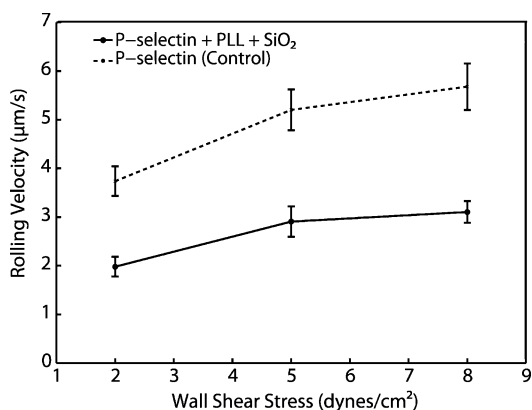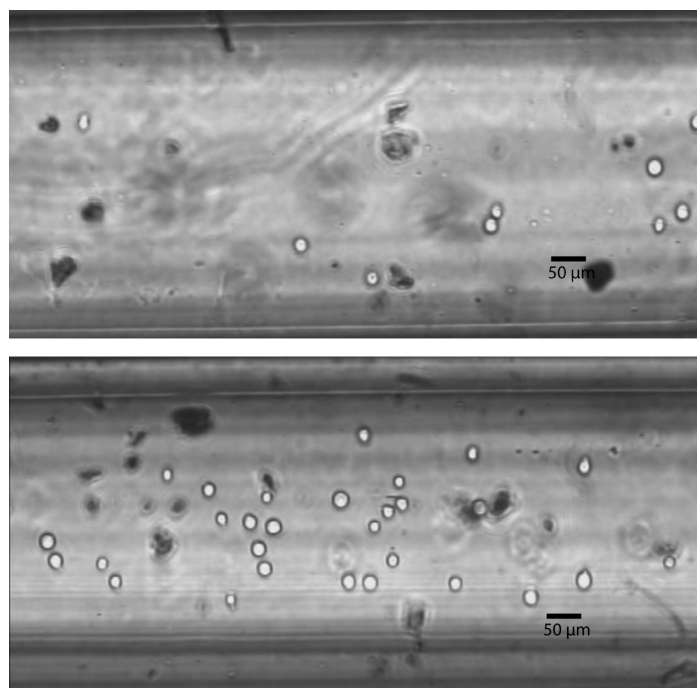

Figure 5. Rolling studies on nanoparticle-coated and control tubes indicated a significantly slower rolling velocity of KG1a cells in nanoparticle-coated tubes. Rolling velocity at each wall shear stress was significantly different when comparing the two surfaces ($P = 0.00021$ (<0.05); $P = 0.00076$ (<0.05); $P = 0.00018$ (<0.05)).

Figure 6. Representative micrograph images captured at 8 dyn/cm^2. Top: P-selectin (control) tube. Bottom: PLL + NP + P-selectin tube.
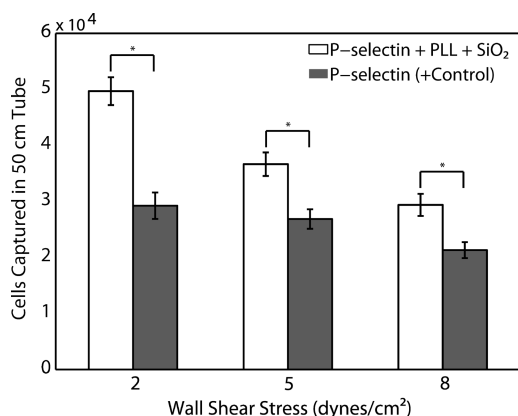
Figure 7. Total number of cells captured in 50 cm long device under varying wall shear stresses: $*P < 0.05$.

contribute to the increased cell capture without P-selectin presence. Titanium(IV) butoxide coating acts exclusively as a NP-immobilizing layer, and the immobilized NPs increase the surface area onto which more P-selectin can bind.

The adhesion of cells to NP surfaces was also tested as a function of shear stress and compared to the control surfaces. In accordance with NP surfaces prepared with PPL, the total number of cells captured on the NP-
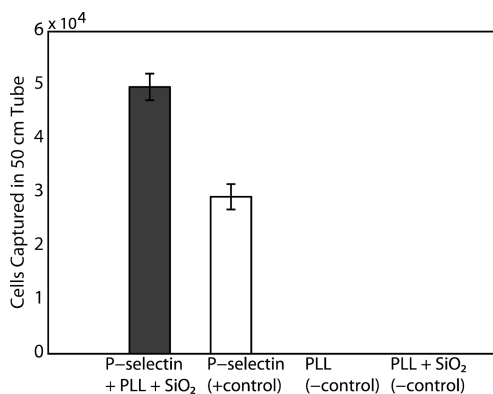

Figure 8. Total number of cells captured on various surfaces at 2 dyn/cm². No cell adhesion was observed in negative controls.
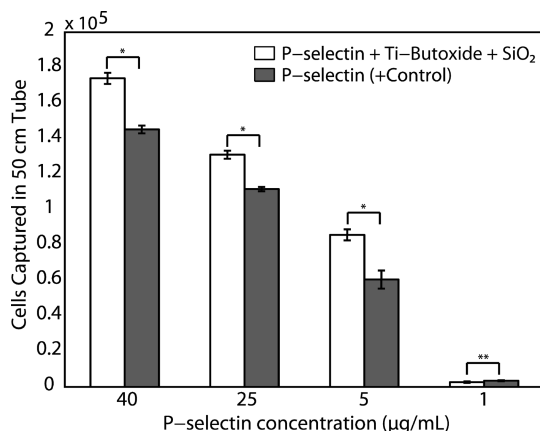

Figure 9. Total number of cells captured in 50 cm long device under a constant wall shear stress of 2 dyn/cm². Negative controls are discussed in text above: $*P < 0.05$; $**P > 0.05$.
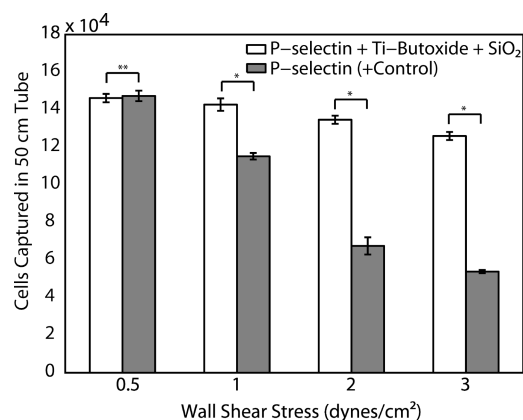

Figure 10. Total number of cells captured in 50 cm long device under varying wall shear stresses. P-selectin incubation concentration was maintained constant at 5 μg/mL: $*P < 0.05$; $**P > 0.05$.

treated surfaces was significantly increased under wall shear stresses above 1 dyn/cm² compared to the control surface without the NP layer ($P < 0.05$) (Figure 10). At the lowest shear stress studied (0.5 dyn/cm²), no significant differences were observed in the total number of cells captured. Furthermore, cells rolling on the NP-treated surface were found to have stronger adhesion, with their rolling velocity appearing significantly slower (Figure 11).

It has been previously shown that titanium and its alloys (TiO₂, titanium(IV) butoxide) possess excellent biocompatibility and hemocompatibility.[19,35−38] Superior hemocompatibility is possibly induced by a number of factors such as low interface energies between the titanium oxide coatings and serums, as well as semiconducting property of the films.[19] Therefore, titanium(IV) butoxide could potentially be an ideal adhesive when coating an implantable device.

CONCLUSIONS

In summary, capture of flowing cells in microtubes coated with NPs was significantly enhanced, thereby increasing the nanoscale surface roughness and total surface area. Using either titanium(IV) bu-
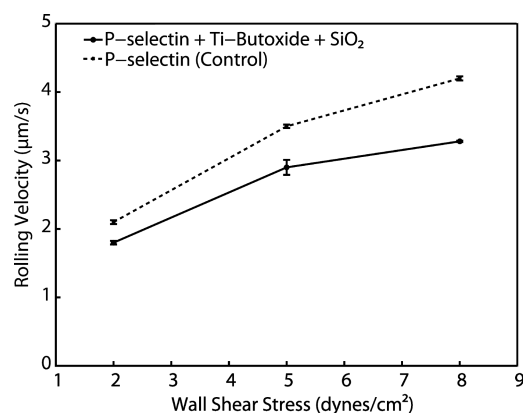

Figure 11. Rolling studies on NP-coated and control tubes indicated a significantly slower rolling velocity of KG1a cells in NP-coated tubes. A statistically significant difference in rolling velocity was found at each shear stress studied.

toxide (inorganic) or PLL (organic) layers as adhesives, NPs were successfully immobilized to create novel nanosurfaces that resulted in enhanced protein adsorption. Upon NP immobilization using the adhesives, the cell rolling velocities and the number of cells captured showed significant enhancement in NP-coated tubes. Negative controls (no P-selectin incubations, blocked with 5% BSA), PLL and PLL with NP-coated surfaces confirmed that the enhancement is only observed when P-selectin is present. In addition, the immunofluorescence quantification indicated significantly higher presence of P-selectin compared to the control tube. Taken together, these results suggest that adhesive-immobilized NP coatings can significantly improve applications to isolate or sort cells using adhesive molecules under flow.

MATERIALS AND METHODS

Preparation of KG1a Cells. KG1a (acute myeloid leukemia) cells were cultured in RPMI media (Mediatech, USA) with 1% L-glutamine (Mediatech, USA) and 10% fetal bovine serum (FBS) (Atlanta Biological, USA). For experiments, cells were isolated from the media and added to Hank's balanced salt solution (HBSS+) (Invitrogen, USA) to a final concentration of 1×10^6 cells/mL.[1]

Preparation of Nanoparticle-Coated Microtube Using Poly-L-lysine. Poly-L-lysine (PLL)$_n$ (0.1% w/v, in water; Sigma-Aldrich, USA) solution was diluted to 2:8 with deionized water. The solution was incubated inside Micro-Renathane tubing (MRE-025, i.d. = 300 μm, length = 50 cm; Braintree Scientific, USA) for 5 min at room temperature. SiO$_2$ nanoparticles (NPs) dispersed in methanol (10−15 nm, 30−31 wt % SiO$_2$, pH 4; Organosilicasol, Nissan Chemicals, USA) were perfused through the tube and incubated for 3 min at room temperature. In order to prevent tube clogging, the tube was flushed with methyl alcohol (Mallinckrodt Chemicals, USA). The tube was stored at room temperature overnight for curing.

Preparation of Nanoparticle-Coated Microtube Using Titanium(IV) Butoxide. Titanium(IV) butoxide (Tyzor TBT, DuPont, USA) solution was diluted to 2:8 with butyl alcohol (Mallinckrodt Chemicals, USA). The solution was incubated within Micro-Renathane tubing (MRE-025, i.d. = 300 μm, length = 50 cm). SiO$_2$ NPs dispersed in methanol (10−15 nm, 30−31 wt % SiO$_2$, pH 4) were perfused through the tube immediately and incubated for 1 min at room temperature. The tube was washed with methyl alcohol to prevent clogging and then stored at room temperature overnight for curing.

Microtube Preparation for Cell Capture and Rolling. Recombinant human P-selectin/Fc Chimera (P-selectin; R&D Systems, USA) at a concentration of 5 μg/mL in phosphate buffered saline (PBS; Invitrogen, USA) was incubated inside the tube for 2 h at room temperature. After washing the tube with PBS, the tubes were incubated with 5% bovine serum albumin (BSA; Sigma-Aldrich, USA) to block nonspecific binding. HBSS+ was pumped through the tube to activate the coated P-selectin.[4,5] For each experiment, four tubes were prepared following the same procedure: P-selectin tube, PLL tube, NP-coated tube, and P-selectin + NP-coated tube.

Cell Capture and Rolling Experiments. Tubes were placed on the stage of an Olympus IX-81 motorized inverted microscope (Olympus America Inc., USA) attached to a CCD camera (Hitachi, Japan). A syringe pump (New Era Pump Systems) was used to control the flow rate of the cell suspension. All images and videos were recorded on high-quality DVD+RW discs for offline analysis.

Fluorescence Microscopy. Tubes were prepared with P-selectin and blocked with 5% BSA, in the same manner as described above. The tubes were incubated with mouse anti human CD62P-Alexa 647 mAb (Serotec, USA) for 2 h. An Olympus IX-81 microscope with Cooke Sensicam QE camera and IP Lab software were used to record the fluorescent images under TRITC mode. Image analysis was performed using ImageJ (NIH) and Excel (Microsoft). The background fluorescence of the tube was subtracted from each reading.

AFM Analysis. AFM images were taken of both NP and control (adhesive only) surfaces. Both surfaces were prepared by steps shown previously on glass slides and washed thoroughly with distilled water.

Data Analysis. Videos from DVD+RW discs were reformatted to 640 × 480 pixels at 29.97 fps with ffmpegX software. Rolling velocities of cells in the tubes were acquired using ImageJ, Excel, and Matlab R2007a (Mathworks). For statistical analysis, paired t test (α = 0.05 level of significance) was used to analyze the data where applicable. Each experimental condition was repeated twice and reported as mean ± SEM values. Immobilized or rolling cells were considered captured. The definition of rolling and the method of estimating the number of cells captured in 50 cm long tube were as previously described.[2,3] Rolling cells were defined as cells rolling at <50% of the calculated hydrodynamic free stream velocity, and cells that remained stationary for more than 10 s were not classified as rolling.

REFERENCES AND NOTES

1. Charles, N.; Liesveld, J. L.; King, M. R. Investigating the Feasibility of Stem Cell Enrichment Mediated by Immobilized Selectins. *Biotechnol. Prog.* **2007**, *23*, 1463–1472.
2. Narasipura, S. D.; Wojciechowski, J. C.; Charles, N.; Liesveld, J. L.; King, M. R. P-Selectin-Coated Microtube for Enrichment of CD34+ Hematopoietic Stem and Progenitor Cells from Human Bone Marrow. *Clin. Chem.* **2008**, *54*, 77–85.
3. Hong, S.; Lee, D.; Zhang, H.; Zhang, Q. J.; Resvick, N. R.; Khademhosseini, A.; King, M. R.; Langer, R.; Karp, J. M. Covalent Immobilization of P-Selectin Enhances Cell Rolling. *Langmuir* **2007**, *23*, 12261–12268.
4. Lord, M. S.; Cousins, B. G.; Doherty, P. J.; Whitelock, J. M.; Simmons, A.; Williams, R. L.; Milthorpe, B. K. The Effect of Silica Nanoparticulate Coatings on Serum Protein Adsorption and Cellular Response. *Biomaterials* **2006**, *27*, 4856–4862.
5. Galli, C.; Coena, M. C.; Hauertb, R.; Katanaevc, V. L.; Gröninga, P.; Schlapbacha, L. Creation of Nanostructures to Study the Topographical Dependency of Protein Adsorption. *Colloids Surf., B* **2002**, *26*, 255–267.
6. Ding, L.; Du, D.; Zhang, X.; Ju, H. Trends in Cell-Based Electrochemical Biosensors. *Curr. Med. Chem.* **2008**, *15*, 3160–3170.
7. Cheng, W.; Ding, L.; Lei, J.; Ding, S.; Ju, H. Effective Cell Capture with Tetrapeptide-Functionalized Carbon Nanotubes and Dual Signal Amplification for Cytosensing and Evaluation of Cell Surface Carbohydrate. *Anal. Chem.* **2008**, *80*, 3867–3872.
8. Hao, C.; Ding, L.; Zhang, X.; Ju, H. Biocompatible Conductive Architecture of Carbon Nanofiber-Doped Chitosan Prepared with Controllable Electrodeposition for Cytosensing. *Anal. Chem.* **2007**, *79*, 4442–4447.

9. Ding, L.; Hao, C.; Xue, Y.; Ju, H. A Bio-Inspired Support of Gold Nanoparticles−Chitosan Nanocomposites Gel for Immobilization and Electrochemical Study of K562 Leukemia Cells. *Biomacromolecules* **2007**, *8*, 1341–1346.

10. Du, D.; Cai, J.; Ju, H.; Yan, F.; Chen, J.; Jiang, X.; Chen, H. Contruction of a Biomimetic Zwitterionic Interface for Monitoring Cell Proliferation and Apoptosis. *Langmuir* **2005**, *21*, 8394–8399.

11. Du, D.; Ju, H.; Zhang, X.; Chen, J.; Cai, J.; Chen, H. Electrochemical Immunoassay of Membrane P-Glycoprotein by Immobilization of Cells on Gold Nanoparticles Modified on a Methoxysilyl-Terminated Butyrylchitosan Matrix. *Biochemistry* **2005**, *44*, 11539–11545.

12. Du, D.; Liu, S.; Chen, J.; Ju, H.; Lian, H.; Li, J. Colloidal Gold Nanoparticle Modified Carbon Paste Interface for Studies of Tumor Cell Adhesion and Viability. *Biomaterials* **2005**, *26*, 6487–6494.

13. Dalby, M. J.; Giannarasa, D.; Riehlea, M. O.; Gadegaarda, N.; Affrossmanb, S.; Curtisa, A. S. G. Rapid Fibroblast Adhesion to 27 nm High Polymer Demixed Nano-Topography. *Biomaterials* **2004**, *25*, 77–83.

14. McKeehan, W. L.; Ham, R. G. Stimulation of Clonal Growth of Normal Fibroblasts with Substrata Coated with Basic Polymers. *J. Cell Biol.* **1976**, *71*, 727–734.

15. Kumar, A.; Liang, Z. Chemical Nanoprinting: A Novel Method for Fabricating DNA Chips. *Nucleic Acids Res.* **2001**, *29*, 2.

16. Yang, Y.; Qu, L.; Dai, L.; Kang, T.; Durstock, M. Electrophoresis Coating of Titanium Dioxide on Aligned Carbon Nanotubes for Controlled Syntheses of Photoelectronic Nanomaterials. *Adv. Mater.* **2007**, *19*, 1239–1243.

17. Chittibabu, K. Photovoltaic Cell. U.S. Patent 2003/0056821, 2003.

18. Campbell, S. Catalysis Support for an Electrochemical Fuel Cell. International Patent WO 2006/002228, 2006.

19. Huang, N.; Yang, P.; Leng, Y. X.; Chen, J. Y.; Sun, H.; Wang, J.; Wang, G. J.; Ding, P. D.; Xi, T. F.; Leng, Y. Hemocompatibility of Titanium Oxide Films. *Biomaterials* **2003**, *24*, 2177–2187.

20. Coradin, T.; Durupthy, O.; Livage, J. Interactions of Amino-Containing Peptides with Sodium Silicate and Colloidal Silica: A Biomimetic Approach of Silicification. *Langmuir* **2002**, *18*, 2331–2336.

21. Wojciechowski, J. C.; Narasipura, S. D.; Charles, N.; Mickelsen, D.; Rana, K.; Blair, M. L.; King, M. R. Capture and Enrichment of CD34-Positive Hematopoietic Stem and Progenitor Cells from Blood Circulation Using P-Selectin in an Implantable Device. *Br. J. Hamaetol.* **2008**, *140*, 673–681.

22. Paterlini-Brechot, P.; Benali, N. L. Circulating Tumor Cells (CTC) Detection: Clinical Impact and Future Directions. *Cancer Lett.* **2007**, *253*, 180–204.

23. Zieglschmid, V.; Hollmann, C.; Bocher, O. Detection of Disseminated Tumor Cells in Peripheral Blood. *Crit. Rev. Clin. Lab. Sci.* **2005**, *42*, 155–196.

24. Allard, W. J.; Matera, J.; Miller, M. C.; Repollet, M.; Connelly, M. C.; Rao, C.; Tibbe, A. G.; Uhr, J. W.; Terstappen, L. W. Tumor Cells Circulate in the Peripheral Blood of All Major Carcinomas but Not in Healthy Subjects or Patients with Nonmalignant Diseases. *Clin. Cancer Res.* **2004**, *10*, 6897–6904.

25. Vona, G.; Sabile, A.; Louha, M.; Sitruk, V.; Romana, S.; Lacour, K. B.; Brechot, C.; Paterlini-Brechot, P. Isolation by Size of Epithelial Tumor Cells: A New Method for the Immunomorphological and Molecular Characterization of Circulating Tumor Cells. *Am. J. Pathol.* **2000**, *156*, 57–63.

26. Went, P. T.; Lugli, A.; Meier, S.; Bundi, M.; Mirlacher, M.; Sauter, G.; Dirnhofer, S. Frequent EpCam Protein Expression in Human Carcinomas. *Hum. Pathol.* **2004**, *35*, 122–128.

27. Nagrath, S.; Sequist, L. V.; Maheswaran, S.; Bell, D. W.; Irimia, D.; Ulkus, L.; Smith, M. R.; Kwak, E. L.; Digumarthy, S.; Muzikansky, A.; Ryan, P.; Balis, U. J.; Tompkins, R. G.; Haber, D. A.; Toner, M. Isolation of Rare Circulating Tumour Cells in Cancer Patients by Microchip Technology. *Nature* **2007**, *450*, 1235–1239.

28. King, M. R.; Western, L. T.; Rana, K.; Liesveld, J. L. Biomolecular Surfaces for the Capture and Reprogramming of Circulating Tumor Cells. *J. Bionic Eng.* in press.

29. Yang, J.; Hirata, T.; Croce, K.; Merrill-Skoloff, G.; Tchernychev, B.; Williams, E.; Flaumenhaft, R.; Furie, B. C.; Furie, B. Targeted Gene Disruption Demonstrates that P-Selectin Glycoprotein Ligand 1 (PSGL-1) Is Required for P-Selectin-Mediated but Not E-Selectin Mediated Neutrophil Rolling and Migration. *J. Exp. Med.* **2001**, *190*, 1769–1782.

30. Moore, K. L.; Patel, K. D.; Bruehl, R. E.; Fugang, L.; Johnson, D. A.; Lichenstein, H. S.; Cummings, R. D.; Bainton, D. F.; McEver, R. P. P-Selectin Glycoprotein Ligand-1 Mediates Rolling of Human Neutrophils on P-Selectin. *J. Cell Biol.* **1995**, *128*, 661–671.

31. Norman, K. E.; Moore, K. L.; McEver, R. P.; Ley, K. Leukocyte Rolling *In Vivo* is Mediated by P-Selectin Glycoprotein Ligand-1. *Blood* **1995**, *86*, 4417–4421.

32. Sackstein, R.; Dimitroff, C. J. A Hematopoietic Cell L-Selectin Ligand That Is Distinct from PSGL-1 and Displays N-Glycan-Dependent Binding Activity. *Blood* **2000**, *96*, 2765–2774.

33. Gautier, C.; Lopez, P. J.; Hemadi, M.; Livage, J.; Coradin, T. Biomimetic Growth of Silica Tubes in Confined Media. *Langmuir* **2006**, *22*, 9092–9095.

34. Gautier, C.; Lopez, P. J.; Livage, J.; Coradin, T. Influence of Poly-L-lysine on the Biomimetic Growth of Silica Tubes in Confined Media. *J. Colloid Interface Sci.* **2007**, *309*, 44–48.

35. Hawkins, K. M.; Wang, S. S. S.; Ford, D. M.; Shantz, D. F. Poly-L-lysine Template Silicas: Using Polypeptide Secondary Structure To Control Oxide Pore Architectures. *J. Am. Chem. Soc.* **2006**, *126*, 9112–9119.

36. Idiris, A.; Alam, M. T.; Ikai, A. Spring Mechanics of Alpha-Helical Polypeptide. *Protein Eng.* **2000**, *13*, 763–770.

37. Lévy, R.; Maaloum, M. Probing Adsorbed Polymer Chains using Atomic Force Microscopy: Interpretation of Rupture Distributions. *J. Phys.: Condens. Matter* **2004**, *16*, 7199–7208.

38. Tirrell, M.; Kokkoli, E.; Biesalski, M. The Role of Surface Science in Bioengineered Materials. *Surf. Sci.* **2002**, *500*, 61–83.

39. Hwang, D. S.; Sim, S. B.; Cha, H. J. Cell Adhesion Biomaterial Based on Mussel Adhesive Protein Fused with RGD Peptide. *Biomaterials* **2007**, *28*, 4039–4046.

40. Bershadsky, A.; Chausovsky, A.; Becker, E.; Lyubimova, A.; Geiger, B. Involvement of Microtubules in the Control of Adhesion-Dependent Signal Transduction. *Curr. Biol.* **1996**, *6*, 1279–1289.

41. Lee, D.; Schultz, J. B.; Knauf, P. A.; King, M. R. Mechanical Shedding of L-Selectin from the Neutrophil Surface during Rolling on Sialyl Lewis x under Flow. *J. Biol. Chem.* **2007**, *7*, 4812–4820.

42. Huang, N.; Yang, P.; Cheng, X.; Leng, Y. X.; Zheng, X. L.; Cai, G. J.; Zhen, Z. H.; Zhang, F.; Chen, Y. R.; Liu, X. H.; Xi, T. F. Blood Compatibility of Amorphous Titanium Oxide Films Synthesized by Ion Beam Enhanced Deposition. *Biomaterials* **1998**, *19*, 771–776.

43. Zhang, F.; Liu, X. H.; Mao, Y. G.; Huang, N.; Chen, Y.; Zheng, Z. H.; Zhou, Z. Y.; Chen, A. Q.; Jiang, Z. B. Artificial Heart Valves: Improved Hemocompatibility by Titanium Oxide Coatings Prepared by Ion Beam Assisted Deposition. *Surf. Coat. Technol.* **1998**, *103−104*, 146–150.

44. Chen, J. Y.; Leng, Y. X.; Tian, X. B.; Wang, L. P.; Huang, N.; Chu, P. K. Antithrombogenic Investigation of Surface Energy and Optical Bandgap and Hemocompatibility Mechanism of Ti(Ta^{+5})O$_2$ Thin Films. *Biomaterials* **2002**, *23*, 2545–2552.

45. Advincula, M. C.; Rahemtulla, F. G.; Advincula, R. C.; Ada, E. T.; Lemons, J. E.; Bellis, S. L. Osteoblast Adhesion and Matrix Mineralization on Sol−Gel-Derived Titanium Oxide. *Biomaterials* **2006**, *27*, 2201–2212.